

Role of Royal Jelly in Alleviation of Toxicity Induced by Silver Nanoparticles in Parotid Gland of Adult Male Albino Rats (Histological and Immunohistochemical Study)

Original
Article

Ghada A. Elsammak, Bassant T. Abd Elbaki and Samar Ramzy Mohamed

Department of Medical Histology and Cell Biology, Faculty of Medicine, Zagazig University, Egypt

ABSTRACT

Introduction: Silver nanoparticles (AgNPs) have widespread commercial application in many products such as home and food products. They lead to various harmful effects.

Aim of the Work: The current work aimed to detect the impact of Silver nanoparticles on parotid gland of adult male albino rats and the possible protective role of Royal Jelly. Royal jelly is the hypopharyngeal and mandibular glands' secretion of worker honeybees to feed the young larvae and queen bee. It has been reported to be antioxidant, antihyperglycemic, immunomodulatory and anti-inflammatory agent.

Materials and Methods: Thirty rats were equally divided into 3 groups: Control group, treated group which received silver nano particles (AgNPs) by I.P. injection at a dose of 2 mg/kg once daily for 28 days and protective group which received AgNPs as the previous dose then received royal jelly orally in gavage in a dose of (1 gm/kg body weight) 3 times a week for 28 days. Tissue malondialdehyde (MDA), tissue superoxide dismutase (SOD) and tissue Amylase were calculated. Specimens of parotid gland were examined by light and electron microscopes. The treated group showed vacuolation of acinar and duct cells, darkly stained nuclei, dilated excretory ducts, congested blood vessels and infiltrating inflammatory cells. Ultrastructurally, there were ill defined organelles, dilated RER, autophagic vacuoles and dark heterochromatic nuclei. Immunohistochemically, there was increased cytoplasmic immunostaining of Bax and increased nuclear and cytoplasmic immunostaining of Ki67 in many acini.

Results: These results were estimated morphometrically and statistically. Royal jelly intake showed improving the parotid gland structure and function. Biochemical and histological parameters showed great improvement. Royal Jelly has an ameliorative effect against Silver nanoparticles-induced parotid gland toxicity.

Conclusion: Royal jelly has a potent antioxidant activity against silver nanoparticles in parotid gland of adult male albino rats.

Received: 09 August 2023, **Accepted:** 03 September 2023

Key Words: Parotid gland, royal jelly, silver nanoparticles.

Corresponding Author: Ghada A. Elsammak, MD, Department of Medical Histology and Cell Biology, Faculty of Medicine, Zagazig University, Egypt, **Tel.** +2 012 223 64470, **E-mail:** ghadaelsammak@hotmail.com

ISSN: 1110-0559, Vol. 47, No. 3

INTRODUCTION

Salivary glands produce protein-rich secretion known as saliva. Saliva helps with speech and food solubility and safeguards the oral mucosa and teeth. Additionally, it generates antimicrobial substances affecting oral bacteria^[1]. Moreover, saliva shares in immune defense due to its antioxidative properties^[2].

Parotid gland (PG), the largest major salivary gland, may be affected structurally and functionally by various factors leading to toxicity^[3]. PG dysfunction leads to xerostomia which is a condition affecting oral tissues causing infection of mucous membranes, altered taste, and talking and chewing difficulties^[4].

Nanotechnology is the science designed at nanoscale (1–100 nm). This science is recently used in numerous fields such as material additives, agriculture and nanomedicine^[5].

Silver nanoparticles (AgNPs) are studied due to their widespread application in a variety of products, including food and home products^[6]. They have strong chemical stability and comparatively low price. Additionally, they have potent antimicrobial properties, making them valuable materials for the drinking water filtration industry. AgNPs also have a variety of uses in medicine, drug delivery, dental biomaterials and catheter coating^[7].

Nanotoxicology is known as the study of nanoparticles' harmful effects^[8]. AgNPs can be consumed directly through

food, water, medications and drug delivery devices. Silver ions are discharged into the blood after ingesting products then accumulate in body organs leading to harmful effects. Compared to other metal nanoparticles such as aluminium, iron, nickel, and manganese, they are more harmful^[9].

The use of bee products for therapeutic purposes is known as apitherapy. Honey, propolis, and RJ are currently recognised as healthy foods on a global scale^[10].

Royal jelly (RJ) is the hypopharyngeal and mandibular glands' secretion of worker honeybees to feed the young larvae and queen bee. It has been reported to be antioxidant, antihyperglycemic, immunomodulatory and anti-inflammatory agent. RJ is composed of several biologically active compounds as proteins, minerals (calcium and iron), fatty acids, free amino acids, sugars and vitamins (riboflavin, niacin and thiamine)^[11].

In addition, it has been demonstrated to have antibacterial and tumoricidal properties, and is frequently found in commercial medications, cosmetics and health foods^[12].

The current study aims to detect any protective impacts of royal jelly on parotid gland toxicity brought on by silver nanoparticles in adult male albino rats.

MATERIALS AND METHODS

Chemicals

Silver nanoparticles

Powder of silver nanoparticles (CAS-No. 7440-22-4) in polyvinylpyrrolidone [PVP] as dispersant with particle size less than 100 nm was acquired from Sigma-Aldrich Chemicals, Cairo, Egypt.

Royal Jelly (RJ) was acquired from Pharco Pharmaceutical, Alexandria, Egypt. It was dissolved in distilled water and stored at 30 °C as a maximum temperature.

Animals

In this study, we utilised thirty healthy adult male Wistar albino rats (3-5 months) (250 and 300 gm weight). They were purchased from the Animal House of the Zagazig University in Zagazig, Egypt's Medicine Faculty. They were kept in carefully regulated lab environments with a 12-hour cycle of darkness and light, at 20 °C temperature, a typical balanced food, and unlimited access to water. The Zagazig University's animal ethics committee approved the use of laboratory animals in accordance with the National Institutes of Health's guidelines.

Nanoparticle characterization

The aqueous dispersion of the nanoparticles was drop-cast onto a copper grid that had been coated with carbon in order to analyse the size and shape of the particles^[13,14]. At the faculty of agriculture at Mansoura University in Egypt, the grid was air dried at room temperature before being observed by a transmission electron microscope (JEOL JEM 1010; Jeol Ltd, Tokyo, Japan) (Figure 1).

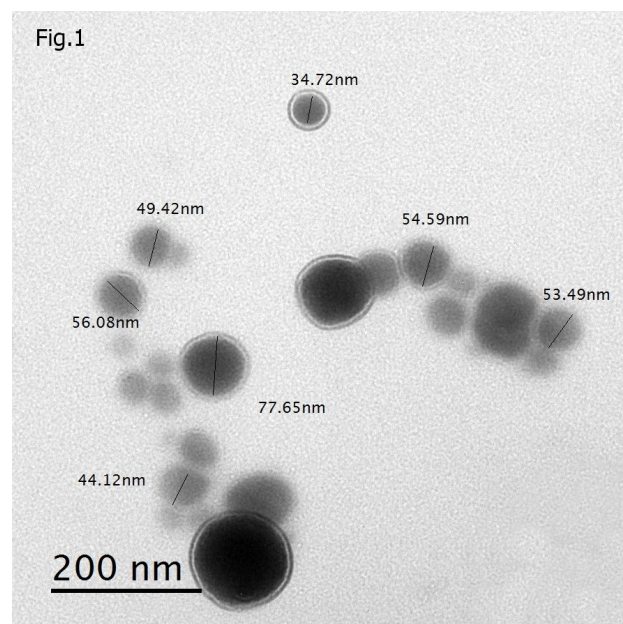


Fig. 1: Transmission electron microscopy showing Silver nanoparticles (AgNps) less than 100 nm size. They were spherical, dispersed and not agglomerated.

Experimental Groups

The animals were equally distributed among three groups (10 rats each):

Group I (Control group): They were equally subdivided into 2 subgroups (5 rats each):

- Subgroup Ia: received no treatment for 28 days.
- Subgroup Ib: received saline solution by intraperitoneal (I.P.) injection for 28 days.

Group II (AgNPs group): Rats received silver nanoparticles (AgNPs) by I.P. injection at a dose of 2 mg/kg once daily for 28 days^[15].

Group III (AgNps- RJ group): Rats received AgNps as the previous dose then received royal jelly orally in gavage in a dose of (1 gm/kg body weight) 3 times a week for 28 days^[16].

At the end of the experiment, the animals were given I.P. injection of 50 mg/kg sodium phenobarbital^[17] to induce anaesthesia then sacrificed by decapitation. After that, each rat had its right and left parotids carefully removed. Samples from each group were inspected by electron and light microscopy.

Biochemical study

Parotid homogenates of the two parotids of five rats from each group were wrapped in aluminium foil and frozen at 80°C and then prepared. Amylase^[18], Superoxide dismutase (SOD) and Malondialdehyde (MDA)^[19] were evaluated in the Biochemistry department of the faculty of medicine at Zagazig University.

Histological study

Light microscope technique

Rat parotid tissue samples were fixed in formalin, dried in varying degrees of ethanol, cleaned in xylene, and then embedded in blocks of paraffin. Sections between four and six micrometres thick were cut by microtome and dyed using:

- i. Hematoxylin and Eosin (H&E) and Mallory's trichrome stain^[20].
- ii. Immunohistochemical staining^[21] for:
 - Bax: apoptosis marker.
 - Ki67: proliferation marker.

For antigen retrieval, sections for immunohistochemical labelling were boiled for 10 minutes at pH 6 in 10 mM citrate buffer. Sections were incubated for 1 hour at room temperature with 6 ml of Bax (p-19) SC-S26, rabbit polyclonal IgG, and a solution of anti-Ki-67 mouse monoclonal Ab diluted 1:100. The sections were then treated for 30 minutes with diluted biotinylated goat anti-rabbit 2ry Ab before being rinsed 3 times in PBS for 5 minutes. After washing the slice in PBS and dipping it in chromogen diaminobenzidine, the reaction products could be seen. After mounting, drying, and counterstaining with Mayer's hematoxylin, the sections were completed.

Finally, stained slides were inspected by LEICA DM500 light microscope at Histology Department of Medicine Faculty at Zagazig University.

Electron microscopic technique

The samples were first fixed in 2.5% glutaraldehyde buffered with 0.1 M phosphate buffer at pH 7.4, followed by a post-fixation in 1% osmium tetroxide, and then analysed by electron microscope. Epoxy resin was utilised to embed after dehydration. The double-stained ultrathin sections were done so with uranyl acetate and lead citrate^[22]. The stained sections were inspected by JEOL JEM 2100 electron microscope at the Electron Microscope unit at Agriculture's faculty, Mansoura University, Egypt.

Morphometric study

At Anatomy Department, Medicine Faculty, Zagazig University, Egypt, 10 non-overlapping fields from various sections of each group were used to evaluate Ki-67 positive nuclei, area percent of collagen fibers and Bax immunostaining by Leica Qwin-500 LTD-software image analysis system (Cambridge, England).

Statistical analysis

"IBM SPSS statistics 21" was used to statistically analyse the histological and biological measurements, and results were then approximated as mean Standard Deviation (SD). To find statistically significant difference between several groups, a one-way analysis of variance (ANOVA) was utilised (*a p value* was judged significant)^[23].

RESULTS

Histological Results

- A. The information acquired from control group's subgroups (Ia and Ib) about outcomes of light and electron microscopy was remarkably similar.
- B. Light microscopic results: Parotid gland sections of Control group stained with H&E revealed closely packed serous acini with vesicular nuclei and striated duct. Narrow septa separated adjacent lobules (Figure 2a). Regarding Silver-nanoparticles group, some sections showed vacuolations of the acinar cells. Some cells had vacuolated cytoplasm with crescent shaped nucleus. Inflammatory cellular infiltration could be seen in between the acini (Figure 2b). Another section showed marked vacuolations of cells lining the acini with dark nuclei. Thickened connective tissue septa appeared around dilated excretory ducts and congested blood vessels. A duct with vacuolated epithelium was present (Figure 2c). Additionally, excessive fibrosis in between the lobules and around dilated congested blood vessel with inflammatory cellular infiltrations appeared (Figure 2d). Concerning AgNps- RJ group, it showed apparently normal acini and ducts except for residual vacuolation and few dark stained nuclei (Figure 2e). In another section of the same group, dilated excretory ducts with vacuolated epithelium and residual congestion was still present (Figure 2f).

Regarding the sections stained with Mallory trichrome stain, the parotid gland of control group exhibited a lack of collagen fibres between the lobules and acini (Figure 3a). Silver-nanoparticles group showed abundant collagen fibers deposited in connective tissue septa around the ducts and blood vessels also (Figure 3b). AgNps- RJ group showed deposition of collagen fibers in moderate amount within as well as in-between the lobules (Figure 3c).

Immunohistochemical staining

Bax-stained parotid gland sections in control group revealed a weak positive immune reaction in the cytoplasm of few acinar cells (Figure 4a). Many of the acini in the Silver-nanoparticles group showed a strong positive cytoplasmic reaction. (Figures 4b, 4c). AgNps-RJ group exhibited a moderate positive cytoplasmic reaction among some acini (Figure 4d).

Ki67-stained sections of parotid gland in control group showed few positive nuclear reactions among few acinar cells (Figure 5a). Silver-nanoparticles group showed increased expression of Ki67 appeared as numerous positive nuclei and moderate cytoplasmic reaction in many acini (Figure 5b). AgNps-RJ group showed some positive nuclei and weak positive cytoplasmic reaction among some acini (Figure 5c).

Electron microscopic results: The acinar cells' nuclei were found to be ovoid euchromatic with a thin rim of heterochromatin in the control group's parotid's ultrathin sections. There were lots of homogenous, electron-dense secretory granules and mitochondria. RER condensed parallel cisternae were also identified. Additionally, apical microvilli were noted. (Figures 6a, b).

Silver nanoparticles group showed features of cellular degeneration. Some cells with abnormal nuclei and periphery condensed heterochromatin were visible. Their cytoplasm showed few secretory granules, markedly dilated cisternae of RER and autophagic vacuoles (Figure 6c). However, some acinar cells showed normal nuclei surrounded by cytoplasm with ill-defined organelles, whereas others had dark heterochromatic nuclei. The cytoplasm also contained some homogenous moderate electron-dense secretory granules as well as some vacuoles that encroached on the nucleus or merged and concentrated on a variety of shapes and sizes. (Figure 6d).

On the other hand, AgNps-RJ group showed that acinar cells expressed relatively normal structure, it retained its normal shape with large irregular euchromatic nuclei. Many small electron-dense granules, rough endoplasmic reticulum, mitochondria and a small number of cytoplasmic vacuoles were also present in their cytoplasm (Figures 6e,f).

Biochemical results

Estimation of the level of tissue amylase enzyme (u/mg)

The mean values of tissue Amylase were 46.35 ± 24.176 in control group, 8.12 ± 5.489 in silver nanoparticle group, 34.61 ± 25.4 in royal jelly group. In contrast to control group, the silver nanoparticle group's data demonstrated a significant statistical decline ($P < 0.001$). The royal jelly group showed high significant increase compared to the silver nanoparticle group. There was not a significant variance between the royal jelly and control groups. (Table 1, Figure 7).

Tissue MDA and SOD among studied groups

The mean values of tissue MDA were 3.963 ± 1.529 in control group, $20.48 \pm .09$ in silver-nanoparticles group, 7.88 ± 4.219 in royal-jelly group. The mean values of tissue SOD were 23.54 ± 3.7 in control group, 9.18 ± 2.5 in silver-nanoparticle group, 19.36 ± 3.63 in royal-jelly group. Between the silver nanoparticle group and the other groups, there was a highly significant difference ($P < 0.001$). There was not a significant distinction between the royal-jelly group and control group. (Table 1, Figure 7).

Morphometrical and Statistical Results

The mean values of area percentage of collagen fibers and BAX immune response, and Ki67 immunopositive cells revealed a significant statistical difference between all groups in research, a significant statistical increase in the silver nanoparticles group compared to the control group, and a significant statistical decrease in the royal-jelly group compared to the silver nanoparticles group (Table 2, Figure 8).

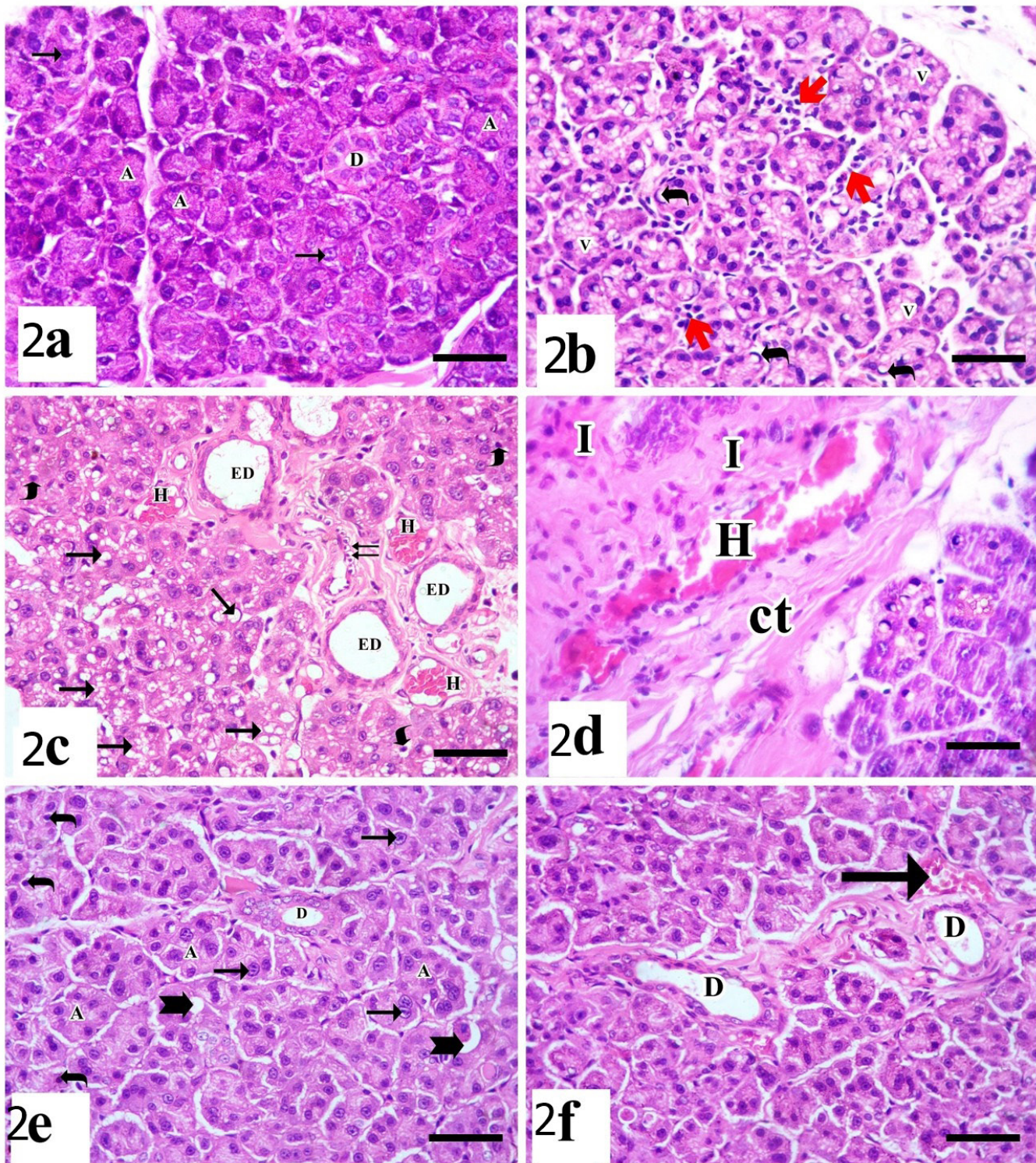


Fig. 2: Photomicrographs of parotid gland sections of: a) Control group showing closely packed serous acini (A) with vesicular nuclei (arrows) and striated duct (D). Narrow septa separate adjacent lobules (arrowhead). (b, c & d) Silver-nanoparticles group showing: b. Section showing vacuolations of the acinar cells (V). Some cells have vacuolated cytoplasm with crescent shaped nucleus (curved arrows). Inflammatory cellular infiltration (red arrow) can be seen in between the acini. c. Another section shows marked vacuolations of the acinar cells (arrows and darkly stained nuclei (curved arrows). Thickened connective tissue septa appeared around dilated excretory ducts (ED) and congested blood vessels (H). A duct with vacuolated epithelium is seen (double arrows). d. Another section reveals excessive fibrosis (ct) in between the lobules around dilated congested blood vessel (H) with inflammatory cellular infiltrations (I). e) AgNps-RJ group shows apparently normal acini (A) and ducts (D). Residual vacuolation (notched arrow) and few dark stained nuclei (curved arrow) can be still noticed. f. Other section shows dilated excretory ducts (D) with vacuolated epithelium (arrowhead) and residual congestion (arrow). (H&E X 400, scale bar 30um)

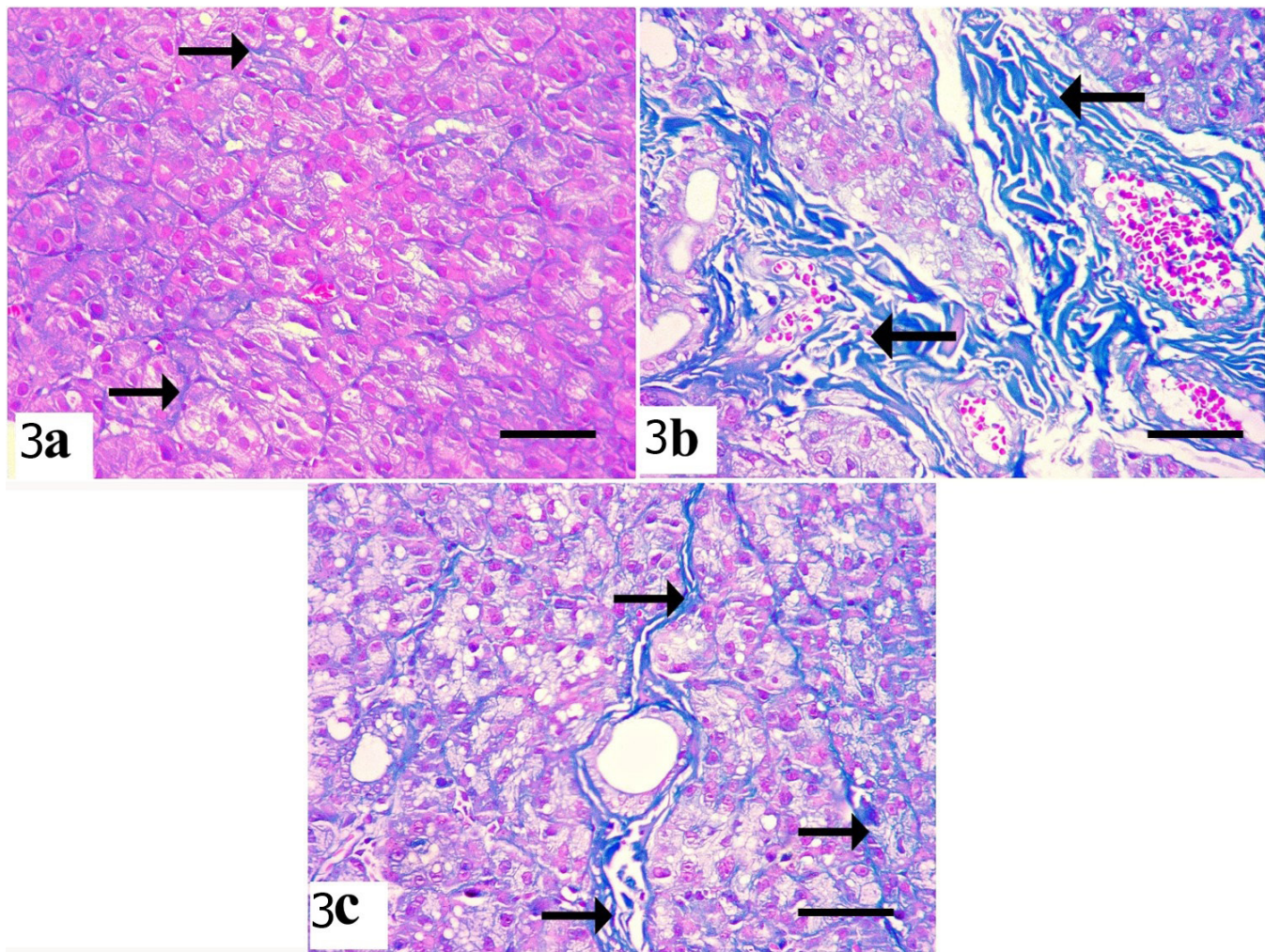


Fig. 3: Photomicrographs of parotid gland sections of: a) Control group reveals scanty collagen fibers (arrows) between lobules and acini. b) Silver-nanoparticles group shows abundant deposition of collagen fibers (arrows) in connective tissue septa around blood vessels and ducts. c) AgNps-RJ group shows deposition of moderate amount of collagen fibers (arrows) between and within lobules. (Mallory's trichrome X 400, scale bar 30um)

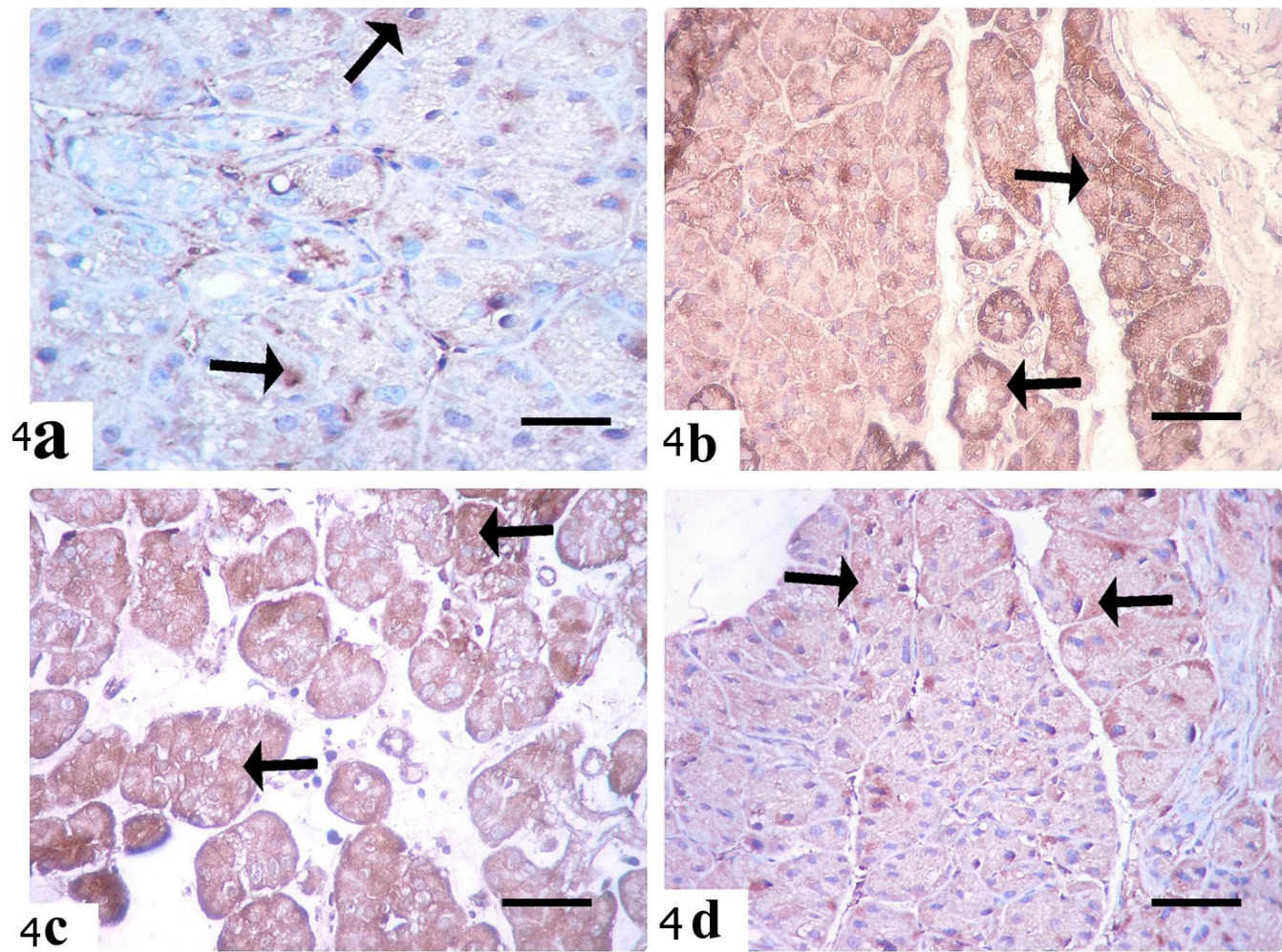


Fig. 4: Photomicrographs of parotid gland sections of: a) Control group showing weak positive cytoplasmic immune reaction (arrows) in few acinar cells. b) Silver-nanoparticles group reveals strong positive cytoplasmic reaction (arrows) in many acini. c) Other section shows also strong reaction in most of acini. d) AgNps-RJ group showing moderate positive cytoplasmic reaction (arrows) among some acini. (BAX x 400, scale bar 30um)

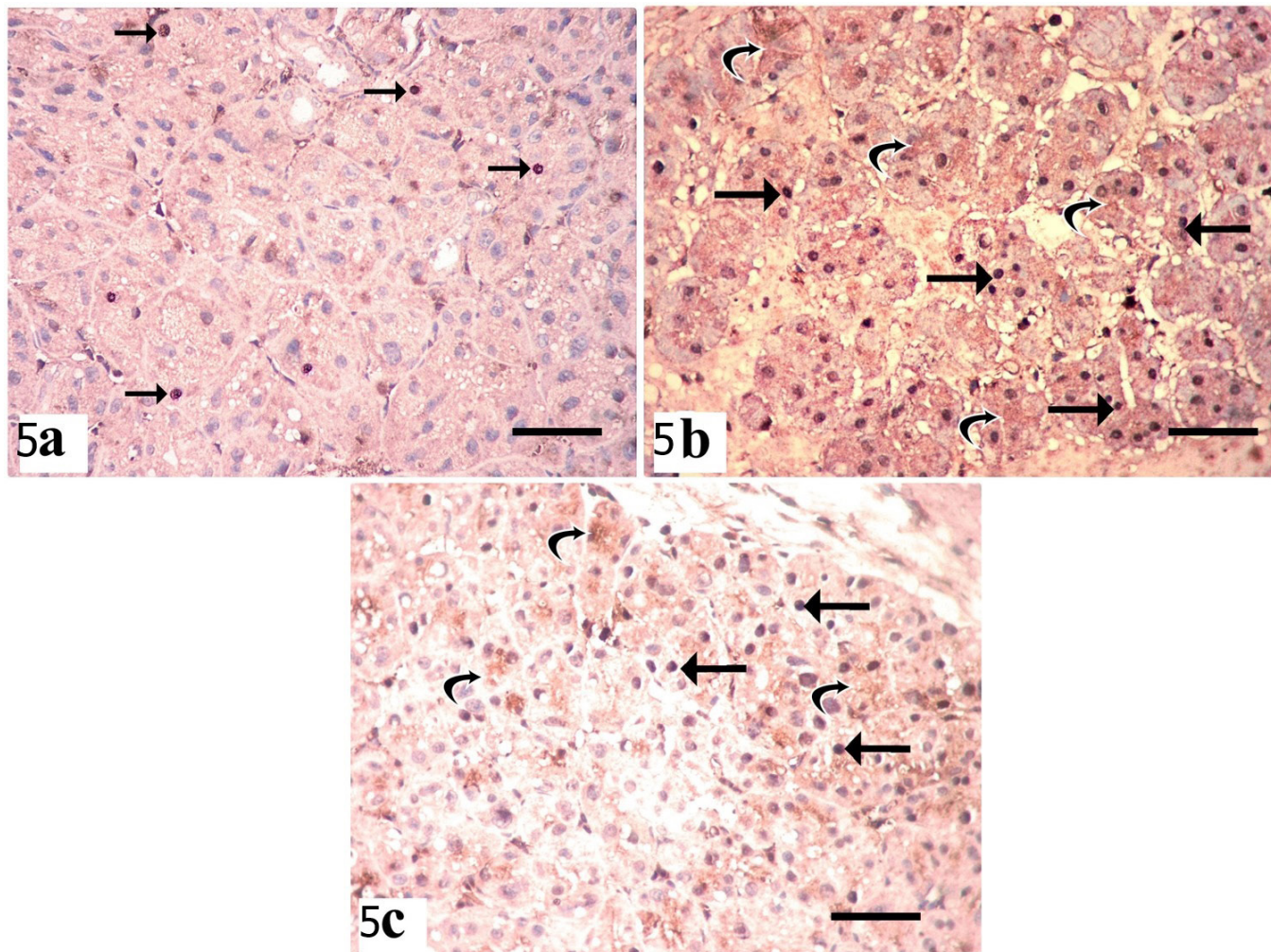


Fig. 5: Photomicrographs of parotid gland sections of: a) Control group showing few positive nuclear reactions (arrows) among few acinar cells. b) Silver-nanoparticles group reveals increased expression of Ki67 appears as numerous positive nuclei (arrows) and moderate cytoplasmic reaction (curved arrows) in many acini. c) AgNps-RJ group showing some positive nuclei (arrows) and weak positive cytoplasmic reaction (curved arrows) among some acini. (Ki67 X 400, scale bar 30um)

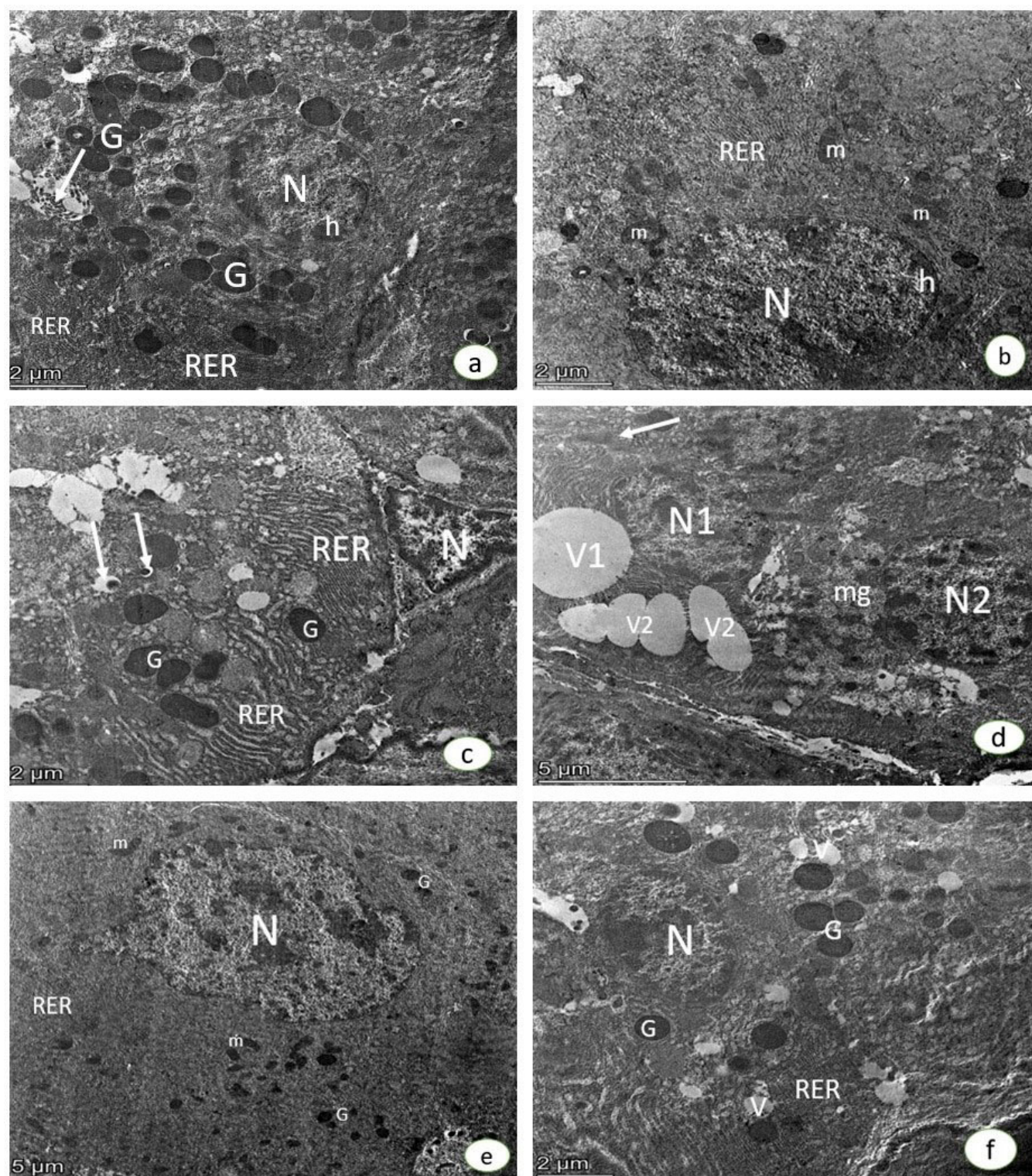


Fig. 6: Electron micrographs of parotid gland ultrathin sections of: (a& b) Control group showing serous acinar cell having oval euchromatic nucleus (N) with a peripheral thin rim of heterochromatin (h). Numerous mitochondria (m), small electron-dense secretory granules (G), and parallel cisternae of rough endoplasmic reticulum (RER) are seen in cytoplasm. Few apical microvilli (arrow) are noticed (TEM Figure a $\times 11000$, Figure b $\times 11000$). Silver nanoparticles treated group revealing signs of degeneration: (c) Acinar cell having irregular nucleus (N) with condensed peripheral chromatin. Few secretory granules (G), markedly dilated cisternae of rough endoplasmic reticulum (RER) and autophagic vacuoles (arrow) are seen. (d) Acinar cells containing a normal nucleus (N1) surrounded by cytoplasm with ill-defined organelles (arrow). Whereas the other demonstrates dark heterochromatic nucleus (N2). Cytoplasm contains homogenous moderate electron-dense cytoplasmic granules (mg). Multiple vacuolations (V1) encroaching on the nucleus of the acinar cell (N1) or merge forming a variety of shapes and sizes (V2) are also observed (TEM Figure c $\times 11000$, Figure d $\times 7800$). (e& f) AgNps-RJ group showing nearly normal serous acini with large irregular euchromatic nucleus (N). Numerous small-sized electron-dense secretory granules (G), mitochondria (m), rough endoplasmic reticulum (RER), and few cytoplasmic vacuoles (v) are seen in cytoplasm (TEM Figure e $\times 5200$, Figure f $\times 11000$).

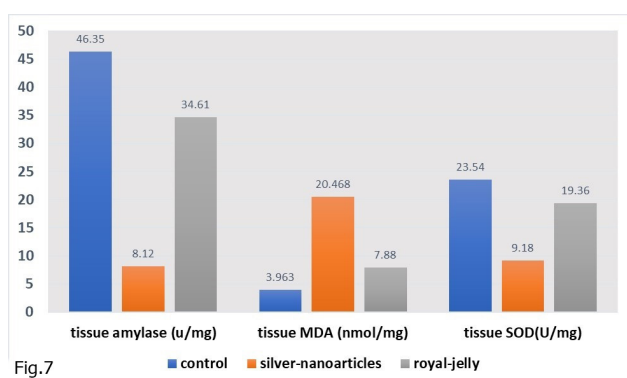


Fig. 7: Comparison between levels of tissue amylase enzyme, MDA & SOD in different groups.

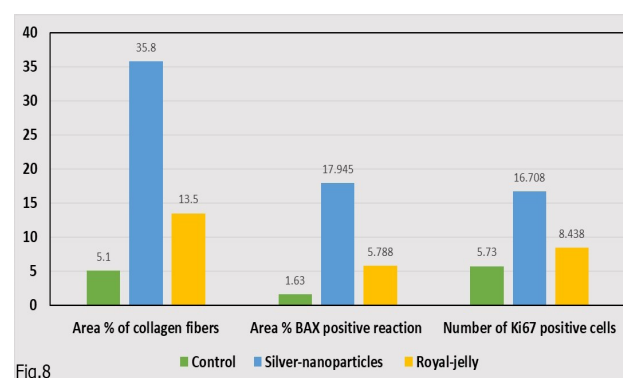


Fig. 8: Comparison between mean area percentage of collagen fibers, BAX immune reaction and mean number of Ki67 positive cells in different studied groups.

Table 1: Comparison between groups regarding the mean values (\pm SD) of tissue amylase, MDA and SOD using ONE WAY ANOVA

| | Control group | Silver-nanoparticle group | Royal-jelly group | F-value | P-value |
|------------------------------|--------------------|---------------------------|--------------------|---------|---------------|
| Tissue amylase enzyme (u/mg) | 46.35 \pm 24.176 | 8.12 \pm 5.489* | 34.61 \pm 25.4 # | 9.1324 | 0.00001 < *** |
| Tissue MDA (nmol/g) | 3.963 \pm 1.529 | 20.468 \pm 6.09 * | 7.88 \pm 4.219 # | 38.98 | 0.00001 < *** |
| Tissue SOD (U/mg) | 23.54 \pm 3.7 | 9.18 \pm 2.5 * | 19.36 \pm 3.63 # | 48.578 | 0.00001 < *** |

*** high significant difference

* High statistical difference compared with control group

High statistical difference compared with silver nanoparticles group

Table 2: Comparison between groups regarding the mean area % of collagen fibers, area % of BAX, and mean number of Ki67 immunostaining using ONE WAY ANOVA

| | Control | Silver-nanoparticles | Royal-jelly | F-value | P-value |
|-------------------------------|------------------|----------------------|--------------------|----------|-------------|
| Area % of collagen fibers | 5.1 \pm 3.178 | 35.8 \pm 14.619* | 13.5 \pm 5.759# | 29.384 | <0.00001*** |
| Area % BAX positive reaction | 0.947 \pm 1.63 | 17.945 \pm 5.56* | 5.788 \pm 2.31# | 57.89259 | <0.00001*** |
| Number of Ki67 positive cells | 5.73 \pm 1.994 | 16.706 \pm 5.55* | 8.438 \pm 3.357# | 21.25305 | <0.0001*** |

*** high significant difference

* High statistical increase compared with control group

High statistical increase compared with silver nanoparticles group

DISCUSSION

The parotid gland was selected as the study's model because it is the largest salivary gland, secreting more than half of all secreted saliva, and is less influenced by drug use^[24].

Silver nanoparticles were the nanoparticles of choice due to their toxic effect on various tissues and their ability to cause pathological diseases like cancer^[25].

IP injection was the chosen method of administration for AgNPs in the current study because it is the most accurate method of exposure^[26]. Additionally, it guarantees that rats receive the correct dose.

Under normal cellular conditions, reactive oxygen species (ROS) are produced and major scavenger enzymes such as superoxide dismutase (SOD) rapidly detoxify them^[27].

One of the most frequent mechanisms of nanoparticle toxicity on organs is the induction of oxidative stress^[28]. Oxidative stress (OS) leads to reduction of intracellular

antioxidants and overproduction of free radicals. This is known as oxidant/antioxidant imbalance which results in lipid peroxidation and antioxidant depletion^[29].

This mechanism explains the biochemical results which revealed significantly increased MDA value which is biomarker of oxidative stress^[30], and decrease in value of SOD which is a protecting enzyme against lipid peroxidation^[31].

In the salivary glands, Amylase is a protein that aids in the beginning of starch digestion. Amylase has been shown to be a biomarker for salivary gland function^[32]. AgNps alter the salivary secretion by altering protein synthesis^[33]. This mechanism confirms the decrease in amylase activity in the AgNps treated group.

Regarding AgNps-treated group's parotid gland sections microscopic examination, there are marked changes such as inflammatory cellular infiltration between the acini, marked vacuolations of acinar and duct cells, dark nuclei, dilated excretory ducts and congested blood vessels.

AgNPs induce apoptosis by the mitochondrial-dependent pathway. AgNPs intake results in the production of ROS leading to cytotoxic and oxidative events ending in apoptosis^[34]. This explains the presence of darkly stained nuclei of acinar cells.

Vacuolations of cells of acini and ducts were noticed. Mahmoud *et al.* attributed them to the accumulated lipid droplets due to unused fatty acids resulting from dysfunction of cells. Lipid droplets combine then form vacuoles^[35]. Samah *et al.* ROS generation has been attributed for the vacuolations. Excessive ROS disrupt cell membranes and cause lipid peroxidation. Therefore, the cell's Na⁺ K⁺ ion pump may be impaired, causing an accumulation of Na⁺ and the entry of water into the cells, which causes swelling and vacuolations^[36].

AgNPs induce pro-inflammatory cytokines, which produce excessive free radicals in cells resulting in DNA damage and cell death^[37]. Thereby, inflammatory reactions like cellular infiltration could be explained.

Excessive ROS lead to vascular dysfunction^[38]. The blood vessels congestion and dilatation occur to transfer large amount of blood to the affected tissues^[39].

The excretory ducts showed dilated lumens due to glandular dysfunction. So, exocytosis is disturbed and thereby, the salivary secretion is accumulated^[40].

Ultrastructurally, Silver nanoparticles treated group revealed marked degenerative changes such as markedly dilated rough endoplasmic reticulum, ill-defined organelles, dark heterochromatic nuclei, electron-dense cytoplasmic granules and autophagic vacuoles.

Nanoparticles are able to cross membranes of cells causing their damage. Overproduction of ROS lead to damage of cell membrane, cytoskeleton and organelles. This explains the presence of ill-defined organelles^[41].

Some researchers claimed that RER dilatation was found as cellular changes prior to apoptosis^[42]. Yasuno *et al.* stated that dilated RER might be attributed to malfunction in the secretory mechanism, then the secreted protein is concentrated inside RER cisternae leading to dilatation^[43].

It is thought that the granules and autophagic vacuoles that contain electron-dense material are lysosomes containing AgNPs. The lysosomes' acidic environment allows the cell to engulf and degrade foreign materials as its main method of defense^[44].

ROS, oxidative stress and transforming growth factor β (TGF- β) are all related. The substantial deposition of collagen fibers in the connective tissue septa, around ducts and blood vessels in the Mallory-stained section of parotid gland in the AgNPs treated group is explained by TGF- β , a potent profibrogenic cytokine that promotes fibrosis^[45].

Bax immunostained sections revealed strong positive cytoplasmic reaction in many acini in the AgNPs treated group. In tissue toxicity, Bax protein is activated by DNA

fragmentation. Bax initiates a series of events that release cytochrome c from the mitochondria, aiding in caspase activation later on leading to programmed cell death^[46].

Ki67 protein is an indicator of cell mitotic activity and proliferation^[47]. Ki67 is found in nuclei of cells undergoing proliferation. It emerges only in cell cycle active phases and absent from cell rest phase G0^[48]. Due to the fact that some immunohistochemistry kits contain (MIB-I), a particular antibody against the Ki67 protein that may identify it in the cytoplasm, other researchers were able to detect Ki67 in the cell's cytoplasm^[49]. Faratian *et al.* observed Ki67 as nuclear and cytoplasmic immunoreexpression in case of breast cancer^[50].

Ki67's other function is repairing damaged DNA. In our study, increased expression of Ki67 appears as numerous positive nuclei and moderate cytoplasmic expression in many acini indicates that the parotid gland is able to resist cell death and to proliferate^[51].

The complicated relationship between cell proliferation and apoptosis is a sign that the parotid gland is still maintaining its normal structure and function^[52].

Antioxidants have two main routes of action: The first one is the elimination of ROS initiators via inhibiting the enzymes involved in ROS production. The second one is the chain breaking mechanism and it involves scavenging free radicals through extra electron donation to neutralize them^[53]. Researchers explained the RJ antioxidant effect by chain breaking mechanism. Also, the two vitamins that make up the majority of composition of RJ are vitamins E and C, which function as potent antioxidants by chain breaking mechanism^[54].

The protective group treated with silver nanoparticles and Royal jelly showed improvement histologically, ultrastructurally and immunohistochemically. This is consistent with the findings of Kanbur *et al.*, who investigated the RJ's ameliorative impact on liver damage caused by paracetamol^[55]. Improvement occurred as RJ is a potent antioxidant and has great ability to scavenge free radicals^[56].

Proline, cystine, and cysteine are only a few of the active amino acids that make up RJ. While cysteine and cystine contribute to the formation of glutathione, an antioxidant intracellularly that neutralises ROS and detoxifies carcinogens^[57], proline protects proteins and membranes against stress^[58]. According to several studies, RJ prevents production of pro-inflammatory cytokines like TnF, IL-1 and IL-6^[59].

Biochemical results of the AgNPs- RJ treated group show improvement as MDA decreased and SOD increased. This comes in accordance with Melliou and Chinou who found that RJ protects the liver by lowering levels of lipid peroxidation^[60].

The stimulation of activity of Amylase in rats' parotid glands treated with Royal jelly indicated improvement of

the salivary gland function. Increased Amylase activity indicated the parotid gland's response to treatment with antioxidants^[61].

Silver nanoparticles with their antibacterial characteristics open new pathways to treat and prevent diseases. However, studies on AgNPs toxicity raise our doubts about their potential risk^[62]. Several studies confirm that RJ has anti-inflammatory, antiaging, antioxidant and antitumor effects. These activities are principally due to bioactive components it contains^[63].

CONCLUSION

The current study provides novel information about Royal Jelly's potent antioxidant activity against the Silver-nanoparticles induced toxicity in adult male albino rat's parotid gland.

CONFLICT OF INTERESTS

There are no conflicts of interest.

REFERENCES

1. Ayuob NN. Histological and immunohistochemical study on the possible ameliorating effects of thymoquinone on the salivary glands of rats with experimentally induced hypothyroidism. *Egyptian Journal of Histology*. 2016; 39(2):125-35. DOI: 10.1097/01.EHX.0000489145.55478.51.
2. Zalewska A, Knaś M, Gińdzieńska-Sieśkiewicz E, Waszkiewicz N, Klimiuk A, Litwin K, Sierakowski S, Waszkiel D. Salivary antioxidants in patients with systemic sclerosis. *Journal of Oral Pathology & Medicine*. 2014; 43(1):61-8. <https://doi.org/10.1111/jop.12084>.
3. Lysik D, Niemirowicz-Laskowska K, Bucki R, Tokajuk G, Mystkowska J. Artificial saliva: challenges and future perspectives for the treatment of xerostomia. *International journal of molecular sciences*. 2019; 20(13):3199. <https://doi.org/10.3390/ijms20133199>.
4. FARD EA, Fallahi B, Karimi M, Beiki D, Saghari M, EMAMI AA, FARD EP, Ansari M, Eftekhari M. Changes in salivary gland function following radioiodine therapy of thyroid diseases: A comparison of high-dose therapy for thyroid cancer and low-dose therapy for benign thyroid disease. *Iranian Journal of Nuclear Medicine*. 2015; 23(1): 1–7. <http://irjnm.tums.ac.ir>.
5. Chen Z, Han S, Zhou S, Feng H, Liu Y, Jia G. Review of health safety aspects of titanium dioxide nanoparticles in food application. *NanoImpact*. 2020; 18:100224. <https://doi.org/10.1016/j.impact.2020.100224>.
6. Kraśniewska K, Galus S, Gniewosz M. Biopolymers-Based Materials Containing Silver Nanoparticles as Active Packaging for Food Applications—A Review. *Int. J. Mol. Sci*. 2020; 21:698. <https://doi.org/10.3390/ijms21030698>.
7. Mitchell MJ, Billingsley MM, Haley RM, Wechsler ME, Peppas NA, Langer R. Engineering precision nanoparticles for drug delivery. *Nature Reviews Drug Discovery*. 2021; 20(2):101-24. <https://doi.org/10.1038/s41573-020-0090-8>.
8. Foldbjerg R, Autrup H. Mechanisms of silver nanoparticle toxicity. *Archives of Basic and Applied Medicine*. 2013; 1(1):5-15.
9. Sardari RR, Zarchi SR, Talebi A, Nasri S, Imani S, Khoradmehr A, Sheshde SA. Toxicological effects of silver nanoparticles in rats. *African Journal of Microbiology Research*. 2012; 6(27):5587-93. <https://doi.org/10.5897/ajmr11.1070>.
10. Aslan Z, Aksoy L. Anti-inflammatory effects of royal jelly on ethylene glycol induced renal inflammation in rats. *International braz j urol*. 2015; 41:1008-13. doi: 10.1590/S1677-5538.IBJU.2014.0470.
11. Karaca T, Uz YH, Demirtas S, Karaboga I, Can G. Protective effect of royal jelly in 2, 4, 6 trinitrobenzene sulfonic acid-induced colitis in rats. *Iranian Journal of Basic Medical Sciences*. 2015;18(4):370. PMID: 26019800
12. Nakajima Y, Tsuruma K, Shimazawa M, Mishima S, Hara H. Comparison of bee products based on assays of antioxidant capacities. *BMC complementary and alternative Medicine*. 2009; 9(1):1-9. <https://doi.org/10.1186/1472-6882-9-4>
13. Amin YM, Hawas AM, El-Batal AI, Elsayed SH. Evaluation of acute and subchronic toxicity of silver nanoparticles in normal and irradiated animals. *British Journal of Pharmacology and Toxicology*. 2015; 6(2):22-38.
14. Lee JH, Kim YS, Song KS, Ryu HR, Sung JH, Park JD, Park HM, Song NW, Shin BS, Marshak D, Ahn K. Biopersistence of silver nanoparticles in tissues from Sprague–Dawley rats. *Particle and fibre toxicology*. 2013; 10(1):1-4. <https://doi.org/10.1186/1743-8977-10-36>
15. El Mahdy MM, Eldin TA, Aly HS, Mohammed FF, Shaalan MI. Evaluation of hepatotoxic and genotoxic potential of silver nanoparticles in albino rats. *Experimental and toxicologic pathology*. 2015; 67(1):21-9. <https://doi.org/10.1016/j.etp.2014.09.005>.
16. El-Alfy NZ, Isa M, Mahmoud MF, Emam A. The protective role of the Royal Jelly against histological effects of endoxan drug on the testis of the male albino mice. *New York Science Journal*. 2013; 6(1):96-101. (ISSN: 1554-0200). <http://www.sciencepub.net/newyork..>
17. Wen L, Gao Q, Ma CW, Ge Y, You L, Liu RH, Fu X, Liu D. Effect of polysaccharides from *Tremella fuciformis* on UV-induced photoaging. *Journal of Functional Foods*. 2016; 20:400-10. <https://doi.org/10.1016/j.jff.2015.11.014>.

18. Caraway WT. A stable starch substrate for the determination of amylase in serum and other body fluids. *American Journal of Clinical Pathology*. 1959; 32:97-9. ISSN (Electronic): 1943-7722 CABI Record Number: 19601400100.
19. Wills ED. Evaluation of lipid peroxidation in lipids and biological membranes. *Biochemical toxicology: a practical approach*. (1987) pp:1-304. NII Article ID10015140229.
20. Kiernan J. *Histological and histochemical methods: theory and practice*. 3rd ed. Arnold publisher. London, New York & New Delhi. (2001) pp: 111-162. DOI: 10.1097/01.EHX.0000424169.63765.ac.
21. Bancroft J, Gamble M. *Theory and Practice of Histological Techniques. Staining methods*. 7th ed. Edinburgh, London, Madrid, Melbourne, New York and Tokyo: Churchill Livingstone. (2008) pp: 263-325. ISBN:978.0443.10279.0.
22. HAYAT M.A.: Chemical fixation. In: *Principles and techniques of electron microscopy: Biological applications*. 4th ed. Edinburg, UK: Cambridge University Press. (2000) pp: 4-85. Doi:10.1006/anbo.20011367.
23. Emsley R, Dunn G, White IR. Mediation and moderation of treatment effects in randomised controlled trials of complex interventions. *Statistical methods in medical research*. 2010;19(3):237-70. <https://doi.org/10.1177/0962280209105014>.
24. Ibrahim SH, Soliman ME, Yehia M. Effect of ciprofloxacin on the submandibular salivary gland of adult male albino rat, a light and electron microscope study. *The Egyptian Journal of Histology* 2004; 27: 339-354. ID: emr-65695.
25. Bakr MM, Al-Ankily MM, Shogaa SM, Shamel M. Attenuating Effect of Vitamin E against Silver Nano Particles Toxicity in Submandibular Salivary Glands. *Bioengineering*. 2021; 8(12):219. <https://doi.org/10.3390/bioengineering8120219>.
26. Minigalieva IA, Katsnelson BA, Panov VG, Privalova LI, Varaksin AN, Gurchich VB, Sutunkova MP, Shur VY, Shishkina EV, Valamina IE, Zubarev IV. *In vivo* toxicity of copper oxide, lead oxide and zinc oxide nanoparticles acting in different combinations and its attenuation with a complex of innocuous bio-protectors. *Toxicology*. 2017; 380:72-93. <https://doi.org/10.1016/j.tox.2017.02.007>.
27. Weijl NI, Hopman GD, Wipkink-Bakker A, Lentjes EG, Berger HM, Cleton FJ, Osanto S. Cisplatin combination chemotherapy induces a fall in plasma antioxidants of cancer patients. *Annals of Oncology*. 1998; 9(12):1331-7. <https://doi.org/10.1023/A:1008407014084>.
28. Song MF, Li YS, Kasai H, Kawai K. Metal nanoparticle-induced micronuclei and oxidative DNA damage in mice. *Journal of clinical biochemistry and nutrition*. 2012; 50(3):211-6. <https://doi.org/10.3164/jcfn.11-70>.
29. Hsu PC, Hour TC, Liao YF, Hung YC, Liu CC, Chang WH, Kao MC, Tsay GJ, Hung HC, Liu GY. Increasing ornithine decarboxylase activity is another way of prolactin preventing methotrexate-induced apoptosis: Crosstalk between ODC and BCL-2. *Apoptosis*. 2006; 11:389-99. DOI: 10.1007/s10495-006-4002-0.
30. Tsikas D. Assessment of lipid peroxidation by measuring malondialdehyde (MDA) and relatives in biological samples: Analytical and biological challenges. *Analytical biochemistry*. 2017; 524:13-30. <https://doi.org/10.1016/j.ab.2016.10.021>.
31. Luangwattananun P, Eiamphungporn W, Songtawee N, Bülow L, Ayudhya CI, Prachayasittikul V, Yainoy S. Improving enzymatic activities and thermostability of a tri-functional enzyme with SOD, catalase and cell-permeable activities. *Journal of biotechnology*. 2017; 247:50-9. <https://doi.org/10.1016/j.jbiotec.2017.03.001>.
32. Leite MF, Nicolau J. Sodium tungstate on some biochemical parameters of the parotid salivary gland of streptozotocin-induced diabetic rats: a short-term study. *Biological trace element research*. 2009; 127:154-63. DOI: 10.1007/s12011-008-8233-5
33. More PR, Pandit S, Filippis AD, Franci G, Mijakovic I, Galdiero M. Silver nanoparticles: bactericidal and mechanistic approach against drug resistant pathogens. *Microorganisms*. 2023;11(2):369. DOI: 10.3390/microorganisms11020369
34. Khan, A.A.; Alanazi, A.M.; Alsaif, N.; Al-Anazi, M.; Sayed, A.Y.; Bhat, M.A. Potential cytotoxicity of silver nanoparticles: Stimulation of autophagy and mitochondrial dysfunction in cardiac cells. *Saudi J. Biol. Sci*. 2021; 28: 2762–2771. doi: 10.1016/j.sjbs.2021.03.021
35. Mahmoud EF, Mahmoud MF, Abd Al Haleem M. Royal Jelly ameliorates oxidative stress and tissue injury in submandibular salivary gland of methotrexate treated rabbits: Immunohistochemical study. *J Am Sci*. 2012; 8:501-8. <https://www.semanticscholar.org/paper/c347991c9c6b60fe>
36. El-Sayed SK, Abo El-Yazed AA, El-Bakary NA, *et al.*: Histological and Immunohistochemical Study of the Effect of Alendronate on the Submandibular Salivary Gland of Adult Male Albino Rat and the Possible Protective Effect of Propolis. *Med J Cairo Univ*. 2018; 86: 3119–3132. <https://doi.org/10.21608/mjcu.2018.59886>

37. Cortese-Krott MM, Münchow M, Pirev E, Heßner F, Bozkurt A, Uciechowski P, Pallua N, Kröncke KD, Suschek CV. Silver ions induce oxidative stress and intracellular zinc release in human skin fibroblasts. *Free Radical Biology and Medicine*. 2009; 47(11):1570-7. <https://doi.org/10.1016/j.freeradbiomed.2009.08.023>
38. Li H, Horke S, Förstermann U. Vascular oxidative stress, nitric oxide and atherosclerosis. *Atherosclerosis*. 2014; 237(1):208-19. <https://doi.org/10.1016/j.atherosclerosis.2014.09.001>
39. Moubarak R. The effect of hypercholesterolemia on the rat parotid salivary gland (histopathological and immunohistochemical study). *Cairo Dental Journal*. 2008; 24(1):19-28.
40. Abdel-Wahhab MA, Hassan NS, El-Kady AA, Khadrawy YA, El-Nekeety AA, Mohamed SR, Sharaf HA, Mannaa FA. Red ginseng extract protects against aflatoxin B1 and fumonisins-induced hepatic pre-cancerous lesions in rats. *Food and Chemical Toxicology*. 2010; 48(2):733-42. <https://doi.org/10.1016/j.fct.2009.12.006>
41. Cayli S, Ocakli S, Senel U, Eyerci N, Delibasi T. Role of p97/Valosin-containing protein (VCP) and Jab1/CSN5 in testicular ischaemia-reperfusion injury. *Journal of molecular histology*. 2016; 47:91-100. <https://doi.org/10.1007/s10735-016-9652-9>
42. Takahashi S, Nakamura S, Domon T, Yamamoto T, Wakita M. Active participation of apoptosis and mitosis in sublingual gland regeneration of the rat following release from duct ligation. *Journal of molecular histology*. 2005; 36:199-205. <https://doi.org/10.1007/s10735-005-1764-6>
43. Yasuno K, Igura S, Yamaguchi Y, Imaoka M, Kai K, Mori K. Pathological examination of spontaneous vacuolation of pancreatic acinar cells in mice. *Journal of toxicologic pathology*. 2019; 32(2):105-9. <https://doi.org/10.1293%2Ftox.2018-0065>
44. Sabella S, Carney RP, Brunetti V, Malvindi MA, Al-Juffali N, Vecchio G, Janes SM, Bakr OM, Cingolani R, Stellacci F, Pompa PP. A general mechanism for intracellular toxicity of metal-containing nanoparticles. *Nanoscale*. 2014; 6(12):7052-61. <https://doi.org/10.1039%2Fnc4nr01234h>
45. Cheresh P, Kim SJ, Tulasiram S, Kamp DW. Oxidative stress and pulmonary fibrosis. *Biochimica et Biophysica Acta (BBA)-Molecular Basis of Disease*. 2013; 1832(7):1028-40. <https://doi.org/10.1016/j.bbdis.2012.11.021>
46. Kulsoom B, Shamsi TS, Afsar NA, Memon Z, Ahmed N, Hasnain SN. Bax, Bcl-2, and Bax/Bcl-2 as prognostic markers in acute myeloid leukemia: are we ready for Bcl-2-directed therapy? *Cancer management and research*. 2018; 10:403. <https://doi.org/10.2147%2FCMAR.S154608>
47. Scholzen T, Gerdes J. The Ki-67 protein: from the known and the unknown. *Journal of cellular physiology*. 2000; 182(3):311-22. [https://doi.org/10.1002/\(sici\)1097-4652\(200003\)182:3%3C311](https://doi.org/10.1002/(sici)1097-4652(200003)182:3%3C311)
48. Jang H, Park CK, Son EJ, Kim EK, Kwak JY, Moon HJ, Yoon JH. Hyalinizing trabecular tumor of the thyroid: diagnosis of a rare tumor using ultrasonography, cytology, and intraoperative frozen sections. *Ultrasonography*. 2016; 35(2):131. <https://doi.org/10.14366%2Fusg.15054>
49. Hirokawa M, Carney JA. Cell membrane and cytoplasmic staining for MIB-1 in hyalinizing trabecular adenoma of the thyroid gland. *The American journal of surgical pathology*. 2000; 24(4):575-8. <https://doi.org/10.1097/0000478-200004000-00013>
50. Faratian D, Munro A, Twelves C, Bartlett JM. Membranous and cytoplasmic staining of Ki67 is associated with HER2 and ER status in invasive breast carcinoma. *Histopathology*. 2009; 54(2):254-7. <https://doi.org/10.1111/j.1365-2559.2008.03191.x>
51. Abdelwahab S, El-Hameed A, Saber E, Sayed A. Role of vitamin A in the healing process of alkali caused corneal injury of adult male albino rat: Histological and immunohistochemical study. *Journal of Medical Histology*. 2017; 1(1):57-68. <https://dx.doi.org/10.21608/jmh.2017.1020.1014>
52. Otsuki T, Shimizu K, Zempo-Miyaki A, Maeda S. Changes in salivary flow rate following Chlorella-derived multicomponent supplementation. *Journal of Clinical Biochemistry and Nutrition*. 2016; 59(1):45-8. <https://doi.org/10.3164%2Fjcfn.16-3>
53. Malekinejad H, Ahsan S, Delkhosh-Kasmaie F, Cheraghi H, Rezaei-Golmisheh A, Janbaz-Acyabar H. Cardioprotective effect of royal jelly on paclitaxel-induced cardio-toxicity in rats. *Iranian journal of basic medical sciences*. 2016; 19 (2):221. <https://doi.org/10.22038/ijbms.2016.6549>
54. Nejati V, Zahmatkesh E, Babaei M. Protective effects of royal jelly on oxymetholone-induced liver injury in mice. *Iranian Biomedical Journal*. 2016; 20(4):229. <https://doi.org/10.7508%2Fibj.2016.04.007>
55. Kanbur M, Eraslan G, Beyaz L, Silici S, Liman BC, Altınordulu Ş, Atasever A. The effects of royal jelly on liver damage induced by paracetamol in mice. *Experimental and Toxicologic Pathology*. 2009; 61(2):123-32. <https://doi.org/10.1016/j.etp.2008.06.003>
56. Cemek M, Aymelek F, Büyükkuroğlu ME, Karaca T, Büyükbek A, Yılmaz F. Protective potential of Royal Jelly against carbon tetrachloride induced-toxicity and changes in the serum sialic acid levels. *Food and chemical toxicology*. 2010; 48(10):2827-32. <https://doi.org/10.1016/j.fct.2010.07.013>

57. Parodi PW. A role for milk proteins and their peptides in cancer prevention. *Current pharmaceutical design*. 2007;13(8):813-28. <https://doi.org/10.2174/138161207780363059>
58. Seminotti B, Leipnitz G, Amaral AU, Fernandes CG, da Silva LD, Tonin AM, Vargas CR, Wajner M. Lysine induces lipid and protein damage and decreases reduced glutathione concentrations in brain of young rats. *International Journal of Developmental Neuroscience*. 2008; 26(7):693-8. <https://doi.org/10.1016/j.ijdevneu.2008.07.011>
59. Watanabe S, Suemaru K, Takechi K, Kaji H, Imai K, Araki H. Oral mucosal adhesive films containing royal jelly accelerate recovery from 5-fluorouracil-induced oral mucositis. *Journal of pharmacological sciences*. 2013;121(2):110-8. <https://doi.org/10.1254/jphs.12181fp>
60. Melliou E, Chinou I. Chemistry and bioactivity of royal jelly from Greece. *Journal of agricultural and food chemistry*. 2005; 53(23):8987-92. <https://doi.org/10.1021/jf051550p>
61. Busch L, Sterin-Borda L, Borda E. Differences in the regulatory mechanism of amylase release by rat parotid and submandibular glands. *Archives of Oral Biology*. 2002; 47(10):717-22. [https://doi.org/10.1016/s0003-9969\(02\)00057-2](https://doi.org/10.1016/s0003-9969(02)00057-2)
62. Khaled H. El-Mesalmy, Mohamed A. Shaheen, Noura H. Mekawy and Fatma Mosa (2020): Effect of Silver Nanoparticles on Testes of Prepubertal Male Albino Rats and the Possible Protective Role of Vitamin E (Histological and Immunohistochemical Study). *Egyptian journal of histology*, 44(2),295-308. <https://dx.doi.org/10.21608/ejh.2020.25855.1261>
63. Moustafa, N. Abdul-Hamid, M. El-Neser, K. And Abu khadra, Am (2020): Protective effect of Alpha lipoic acid and Royal Jelly against side effect of cyclophosphamide in testis of male albino rats. *Egyptian journal of histology*,43(2),539-553. <https://dx.doi.org/10.21608/ejh.2019.16643.1167>

الملخص العربي

دور غذاء ملكات النحل في التخفيف من السمية الناتجة عن جزيئات الفضة الدقيقة في الغدة النكفية لذكور الجرذان البيضاء البالغة (دراسة نسيجية وكيميائية مناعية)

غادة السماك، بسنت عبد الباقي، سمر رمزي

قسم علم الأنسجة الطبية وعلم الأحياء الخلوية، كلية الطب، جامعة الزقازيق، مصر

المقدمة: جزيئات الفضة الدقيقة لها تطبيقات تجارية واسعة النطاق في عدد من المنتجات ، مثل المواد الغذائية والمنتجات المنزلية تؤدي إلى تأثيرات ضارة مختلفة. غذاء ملكات النحل هو إفراز البلعوم والغدد السفلية لنحل العسل العامل لإطعام اليرقات الصغيرة وملكة النحل. تم الإبلاغ عن أنه مضاد للأكسدة ، خافض لفرط سكر الدم ، عامل مناعي ومضاد للالتهابات.

الهدف : هدفت الدراسة الحالية إلى الكشف عن تأثير جزيئات الفضة الدقيقة على الغدة النكفية لذكور الجرذان البيضاء البالغة والتأثير الوقائي المحتمل لغذاء ملكات النحل.

المواد والطرق المستخدمة: تم تقسيم ثلاثين جرذاً بالتساوي إلى ٣ مجموعات: المجموعة الضابطة و المجموعة المعالجة التي تلقت جزيئات الفضة الدقيقة بواسطة الحقن بجرعة ٢ مجم / كجم مرة واحدة يومياً لمدة ٢٨ يوماً والمجموعة الواقية التي تلقت جزيئات الفضة الدقيقة كجرعة سابقة ثم تناولت غذاء ملكات النحل عن طريق الفم بجرعة (١ جم / كجم من وزن الجسم) ٣ مرات في الأسبوع لمدة ٢٨ يوماً . تم حساب SOD، MDA و Amylase في الأنسجة وتم فحص عينات الغدة النكفية بواسطة المجاهر الضوئية والإلكترونية.

النتائج: أظهرت المجموعة المعالجة تفريراً لخلايا الحوصلات والقناة ، ونواة ملطخة باللون الداكن ، وقنوات إفرازية متوسعة ، وأوعية دموية محتقنة وخلايا التهابية متسللة. الفحص بواسطة المجهر الإلكتروني أظهر عضيات غير محددة ، و الشبكة الإندوبلازمية الخشنة متوسعة ، وفجوات تلقائية ونواة مغايرة اللون داكنة. من الناحية المناعية ، كان هناك زيادة في رد الفعل المناعي لل Bax في السيتوبلازم و لل Ki67 في النواة و السيتوبلازم. تم تقدير هذه النتائج شكلياً وإحصائياً

الاستنتاج: أظهر تناول غذاء ملكات النحل تحسن في بنية الغدة النكفية ووظيفتها. أظهرت المؤشرات البيوكيميائية والنسجية تحسناً كبيراً. غذاء ملكات النحل له تأثير محسّن ضد سمية الغدة النكفية التي تسببها جزيئات الفضة الدقيقة.